


Adequacy of pseudo-direct georeferencing of terrestrial laser scanning data for coastal landscape surveying against indirect georeferencing

Marion Jaud ^a, Pauline Letortu^b, Emmanuel Augereau^a, Nicolas Le Dantec^{a,c}, Mickaël Beauverger^a, Véronique Cuq^b, Christophe Prunier^a, Réjanne Le Bivic^a and Christophe Delacourt^a

^aLaboratoire Domaines Océaniques – UMR 6538, Université de Bretagne Occidentale, IUEM, Technopôle Brest-Iroise, Plouzané, France;

^bLETG-Brest Géomer – UMR 6554, Université de Bretagne Occidentale, IUEM, Technopôle Brest-Iroise, Plouzané, France; ^cCEREMA - Centre d'Etudes et d'expertise sur les Risques, l'Environnement, la Mobilité et l'Aménagement, DTecEMF, Plouzané, France

ABSTRACT

The georeferencing process is crucial to the accuracy of terrestrial laser scanner (TLS) data, in particular in the context of diachronic studies relying on multi-temporal surveys. The use of Ground Control Points in the georeferencing process can however be complex when confronted with the practical constraints of coastal surveying. A simple and quick alternative method called “pseudo-direct georeferencing” is proposed in the present paper. This method involves internal inclinometers to measure roll and pitch angles and a centimetric GPS to measure the position of the TLS center and the position of one backsight target. When assessing the transformational uncertainty by using a set of independent ground validation points for both classical indirect and proposed pseudo-direct methods, we respectively obtain root mean square errors of 4.4 cm for the indirect method and 3.8 cm for the pseudo-direct method.

ARTICLE HISTORY

Received 20 February 2017

Accepted 22 February 2017

KEYWORDS

Terrestrial laser scanning; coastal monitoring; direct georeferencing; indirect georeferencing; multi-temporal surveys; geomorphological evolution

Introduction

Coastal landscapes are shaped by a set of forcing factors, highly variable both in time and location, making the littoral zone a very dynamic environment. A good understanding of this hydro-geomorphological system requires considering a range of time scales from geological to historical, seasonal and events scale (especially to account for extreme events) as well as different spatial scales from regional (kilometers) to local and fine (centimeters). Coastal morphodynamics therefore needs high spatial resolution and high precision monitoring, but also monitoring at a high frequency (e.g. before and after storm events, and ideally at each low tide during the storm) with extensive spatial coverage. Furthermore, working with datasets georeferenced in absolute coordinates and high absolute accuracy in 3D positioning are necessary to combine multisource data, to carry out diachronic analyses in order to study evolution trends or even to easily share results with coastal stakeholders.

The most basic method for coastal landscape surveying is the GPS or tacheometer pole measurement, a point-wise method associated with low spatial resolution and therefore strong uncertainties. Structure-from-Motion photogrammetric surveys from unmanned aerial vehicles (UAVs) are an emerging alternative to provide high resolution topography (Delacourt et al., 2009; Harwin & Lucieer, 2012; Mancini et al., 2013).

Among other topographic survey instruments, terrestrial laser scanners (TLSs) are convenient since they allow acquisitions at high temporal and spatial resolution with rather limited constraints: the equipment is very portable and the scan positions are defined by the user. TLS data, combined with data from other sources (high resolution satellite, aerial or UAV imagery, photogrammetry, Differential GPS [DGPS] survey, etc.), is thus a key asset for diachronic surveys, which are essential for coastal monitoring.

The TLS technique has been widely used in the study of coastal mass transfers to

- analyze rock falls including those affecting coastal cliffs (Abellán et al., 2014; Kuhn & Prüfer, 2014; Letortu et al., 2015; Quinn, Rosser, Murphy, & Lawrence, 2010; Rosser, Brain, Petley, Lim, & Norman, 2013; Rosser, Petley, Lim, Dunning, & Allison, 2005);
- quantify changes on beach sediment budget, dune and tidal marsh (Leroux, 2013; Lim, Dunning, Burke, King, & King, 2015; Nield, Wiggs, & Squirrell, 2011; Pietro, O'Neal, & Puleo, 2008; Schubert, Gallien, Majd, & Sanders, 2015).

Paffenholz (2012) considers three approaches for georeferencing 3D point clouds, the raw output generated by a TLS:

- (1) indirect georeferencing via ground control points (GCPs), using targets, either fixed

positioned or temporally placed before each survey, that are measured with an independent method (GPS, theodolite) (Lague, Brodu, & Leroux, 2013; Alba et al., 2007; Letortu et al., 2015);

- (2) direct georeferencing, using the internal or external sensors attached to the TLS in order to directly provide the required registration parameters (Lichti & Gordon, 2004; Paffenholz, 2012; Reshetyuk, 2009; Scaioni, 2005);
- (3) cloud-matching techniques using overlapping parts of point clouds (Besl & McKay, 1992; Olsen, Johnstone, Driscoll, Ashford, & Kuester, 2009; Olsen, Johnstone, Kuester, Driscoll, & Ashford, 2011; Schürch, Densmore, Rosser, Lim, & McArdell, 2011). Registration uncertainty may be assessed comparing fixed points in datasets as buildings, roads, etc. This data-driven approach is only mentioned here without further details as it relies on prior (direct or indirect) georeferencing of an initial point cloud in order to obtain absolute georeferencing for the subsequent surveys.

When defining an optimized protocol for TLS surveying applicable to coastal environment monitoring, the following practical constraints are relevant:

- foreshore accessibility is time-limited because of tides, which restricts the number of scans that can be performed and thus imposes compromising between survey area for coverage purpose and scan overlap for co-registration purpose;
- the TLS tripod may have to be placed on undrained sands, in the absence of a better option, and thus be subject to settling, in which case assessing the position and inclination of the TLS device becomes crucial;
- adequate positioning of the reflective targets may not be possible in certain areas (partial masking of satellite constellation at the cliff foot, submerged zone, masking by rocks, stranded seaweeds, etc.);
- setting up a fixed network of GCPs or permanent geodetic marks for georeferencing purpose is challenging because the TLS is generally located on the foreshore, which is subject to significant topographic changes (seasonal and even event-driven variations in beach level), in addition to tampering risks due to the high frequentation of coastal sites.

Such constraints call for a time-efficient protocol for TLS data acquisition in coastal environments. In particular, setting up the targets used as GCPs and measuring their position is a time-consuming step, especially with respect to the scanning speed of current TLS technology.

The quality of the georeferencing is a key issue not only for TLS surveys but also for Mobile Laser Scanning

surveys (Alho et al., 2011; Barber, Mills, & Smith-Voysey, 2008; Kukko, Kaartinen, Hyyppä, & Chen, 2012), which are highly dependent on the positioning and inclination angle measurements. In recent years, significant progress has been made in sensor technology, improving data reliability and reducing acquisition time. Many studies address the comparison of georeferencing techniques for TLS data. However, these studies mainly focus on architectural surveying (Alba, Giussani, Roncoroni, & Scaioni, 2007), civil surveying (Scaioni, 2005), landslide surveying (Giussani & Scaioni, 2004; Kasperski et al., 2010), for which purposes operational constraints and requirements are quite different from those for coastal monitoring. This paper reports on an improvement to the surveying protocol, precisely a reduction in survey duration without affecting georeferencing accuracy. After a brief theoretical description of TLS data registration, this paper presents a field survey where both methods – classical (indirect-georeferencing) and alternative (pseudo-direct georeferencing) – are tested. The results of both methods are then compared and discussed.

Background on TLS data registration

Coordinate systems definition and transformational uncertainty

During data acquisition, the position of an object which has reflected the laser beam is defined relatively to the TLS position knowing the slant range ρ (radial distance), the azimuthal angle α and the inclination angle β (Figure 1). The transformation from spherical coordinates to Cartesian coordinates is given by Equation (1):

$$\begin{pmatrix} x \\ y \\ z \end{pmatrix} = \begin{pmatrix} \rho \cos \beta \cos \alpha \\ \rho \cos \beta \sin \alpha \\ \rho \sin \beta \end{pmatrix} \quad (1)$$

The position of the measured points is thus expressed in a local coordinate system associated with the sensor, generally referred in literature and further mentioned as Intrinsic Coordinate System (ICS). The ICS is defined by the position of the TLS reference point and the orientation of the TLS axes (Figure 1).

To exploit TLS datasets for (1) multi-temporal or multi-sensor comparisons, (2) integration with other geospatial data and (3) diffusion to stakeholders, they need to be registered in a common reference system.

Georeferencing consists in transforming the registration of the point cloud from the ICS into an absolute or Global Coordinate Systems (GLCS), generally associated to a geodetic datum. This transformation is associated with the matrix operator M_{IGL} (Figure 1), a unique combination of a translation and a rotation. Thus, a set of six transformation parameters is required for this registration.

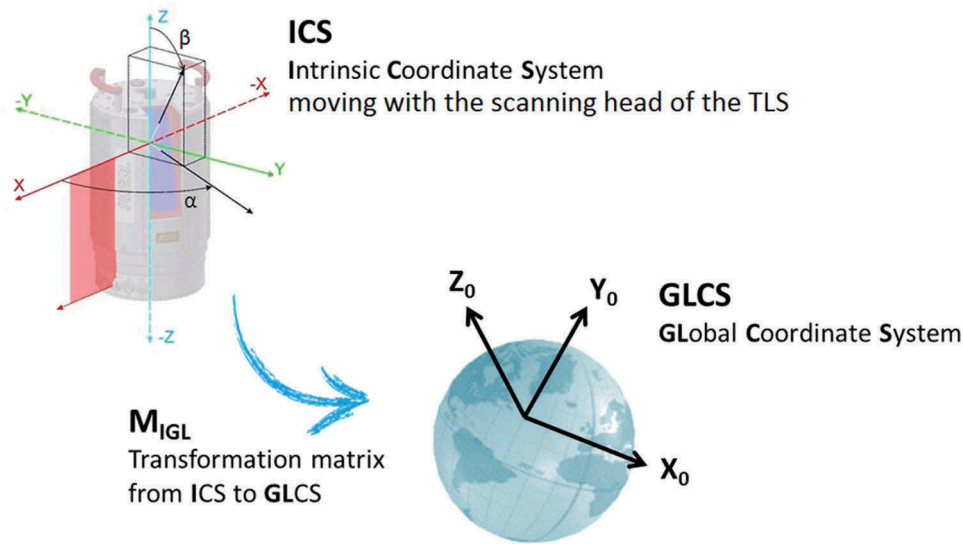


Figure 1. Definition of the coordinates systems.

The error in the final TLS dataset is due to various factors affecting the measurement and the processing. A complete description of sources of uncertainty in TLS data can be found in the work by Paffenholz (2012) and Cuartero, Armesto, Rodríguez, and Arias (2010). The sole focus of this study is on transformational uncertainty, i.e. the error induced by the applied georeferencing method. Random and systematic errors of the TLS, environmentally induced errors or object-related errors are not addressed in this paper.

Indirect georeferencing

This method is widely adopted for high precision measurement applications. It is based on registration of each point cloud using a set of well-spread reflective targets, serving as GCPs. Their coordinates have to be known both in ICS and in GLCS. Their position in GLCS is measured by differential GPS or tacheometer, while their position in ICS is obtained with the TLS by semiautomatic detection and re-scanning at very fine spatial resolution.

During the post-processing, the six parameters of rotation and translation allowing projecting the 3D point cloud from ICS to GLCS are computed from the coordinates of the GCPs in both coordinate systems. A minimum of three GCPs has to be measured for each scan, but in practice a higher number of GCPs is generally used since redundancy improves the reliability of registration (Alba & Scaioni, 2007; Reshetuk, 2009).

A least squares algorithm is applied to compute the transformation matrix M_{IGL} providing the best fit between GCPs position in both coordinate systems.

Direct georeferencing

The M_{IGL} matrix can be decomposed into a rotation and a translation. The transformation of a point p

from scanner space, with coordinates (x, y, z) in the ICS, to the corresponding point P , with coordinates (X, Y, Z) in the GLCS is given by Equation (2):

$$\begin{bmatrix} X \\ Y \\ Z \end{bmatrix}_{GLCS} = \begin{bmatrix} X_0 \\ Y_0 \\ Z_0 \end{bmatrix}_{GLCS} + R \begin{bmatrix} x \\ y \\ z \end{bmatrix}_{ICS} \quad (2)$$

with

$R =$

$$\begin{bmatrix} \cos\psi \cos\theta & -\sin\psi \cos\theta + \cos\psi \sin\theta \sin\varphi & \sin\psi \sin\theta + \cos\psi \sin\theta \cos\varphi \\ \sin\psi \cos\theta & \cos\psi \cos\theta + \sin\psi \sin\theta \sin\varphi & -\cos\psi \sin\theta + \sin\psi \sin\theta \cos\varphi \\ -\sin\theta & \cos\theta \sin\varphi & \cos\theta \cos\varphi \end{bmatrix} \quad (3)$$

where φ , θ and ψ are the roll, pitch and yaw angles of the TLS in the GLCS and

(X_0, Y_0, Z_0) are coordinates in GLCS of the TLS center position.

In the literature (Alba & Scaioni, 2007; Lichti & Gordon, 2004; Scaioni, 2005), “direct georeferencing” generally refers to a method analogous to total station survey, meaning that the TLS is leveled and centered over a known point by an optical plummet. Setting up the TLS over a known location reduces the unknown transformation parameters to three angles. If leveling the TLS, it is hypothesized that $\varphi = \theta = 0$. The orientation in the horizontal plane (i.e. azimuthal angle ψ) is carried out by a pointing system (telescopic sight) or by measuring a target.

With the development of mobile scanning, the concept of direct georeferencing is changing. Commercially available TLS are now indeed generally equipped with internal positioning sensors, compasses, inclinometers and gyroscopes. Also, direct georeferencing now implies real-time georeferencing.

In this paper, “direct georeferencing” refers only to approaches using internal sensors (or external sensors attached to the TLS) directly providing, in real-time,

the six rotation and translation parameters. As using a scope mounted on the TLS or measuring a tie point implies post-processing registration of the point cloud, these methods are not considered in this paper as direct georeferencing methods, but as “pseudo-direct georeferencing methods”.

Field test survey for comparison of georeferencing methods

Experimental setup

A test survey was carried out in July 2015 to compare the different georeferencing methods herein considered. The selected test area is the beach of Porsmilin (Figure 2), located near Brest (France). Various surveys (topography, bathymetry and hydrodynamics) are regularly performed to monitor this beach, which is one of the sites of the National Observation System DYNALIT.

In the present study, the TLS is a Riegl® VZ-400. For this survey configuration, TLS acquisition involves a 360° horizontal and 100° (from 30° to 130°) vertical scan with an angular resolution of 0.04° in both directions, providing a dense 3D point cloud distributed over the scanned area. With the aforementioned parameters, a full scan is completed in 9 min and generates more than 22.5 million points. Taking advantage of existence of a geodetic marker on the site of Porsmilin to set up our GPS reference station and use Real-Time Kinematic (RTK) GPS positioning, centimetric positioning accuracy can be achieved. At sites without geodetic points, post-processing kinematics may be used for GPS data in order to achieve the same positioning accuracy. For this test survey, 28 targets were distributed around the TLS standpoint. These targets are reflective cylinders 10 cm in diameter and 10 cm in height.

The Riegl® VZ-400 TLS can automatically identify reflective targets in the point cloud. The results are then manually checked before programming the TLS to perform a fine scan of the targets to precisely measure their centroid.

The survey is controlled via a PC. Point cloud capture and the following georeferencing steps are

performed with the RiScan Pro® software (Riegl®, Austria).

Indirect georeferencing

Indirect georeferencing is the most traditional method to register stationary TLS data (Bitelli, Dubbini, & Zanutta, 2004; Earlie, Young, Masselink, & Russell, 2015; Jaud et al., 2011). Creating steady known locations for placing targets can be challenging in the coastal environment. Therefore, the configuration of the targets network changes from one session to the next.

Typically, 8–15 reflective targets (depending on the complexity of the area) are spread throughout the scanned scene. For the present survey, 14 reflective targets (depicted by red crosses in Figure 3) were used as GCPs and taken into account for the indirect georeferencing process. In parallel, 14 distinct reflective targets (depicted by blue dots in Figure 3) served as ground validation points (GVPs). These GVPs were used as calibration points to assess the georeferencing uncertainties.

Depending on the size and the topography of the scanning scene, placing GCPs, measuring their position in GLCS and gathering them up may be a time-consuming task. Moreover, the fine-scan process is one of the longest steps of a TLS acquisition. Nevertheless, increasing the number of GCPs improves the global redundancy of the observations, thus reducing the impact of target positioning errors.

Pseudo-direct georeferencing

“Pseudo-direct georeferencing” qualifies an alternative referencing method, for the most part based on the methods proposed by Reshetyuk (2009) and Mårtensson, Reshetyuk, and Jivall (2012). These methods are themselves largely based on a georeferencing approach analogous to procedure used for total station survey (Alba & Scaioni, 2007; Lichti & Gordon, 2004; Scaioni, 2005). The TLS is centered over a known point and precisely leveled.

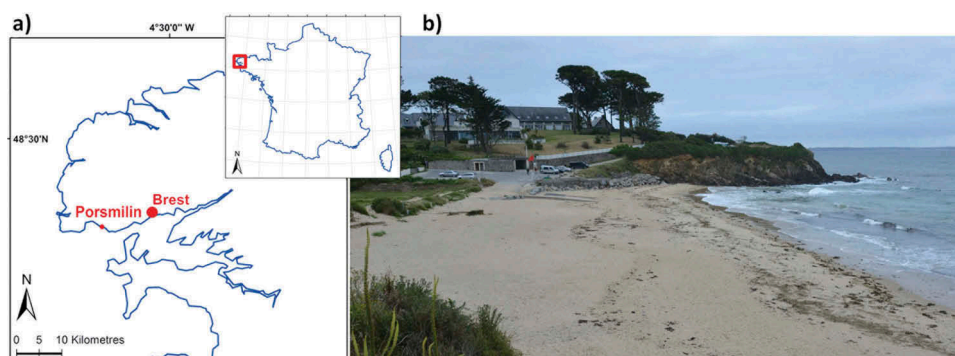


Figure 2. (a) Location map of the study area. (b) The test area: The beach of Porsmilin (France).

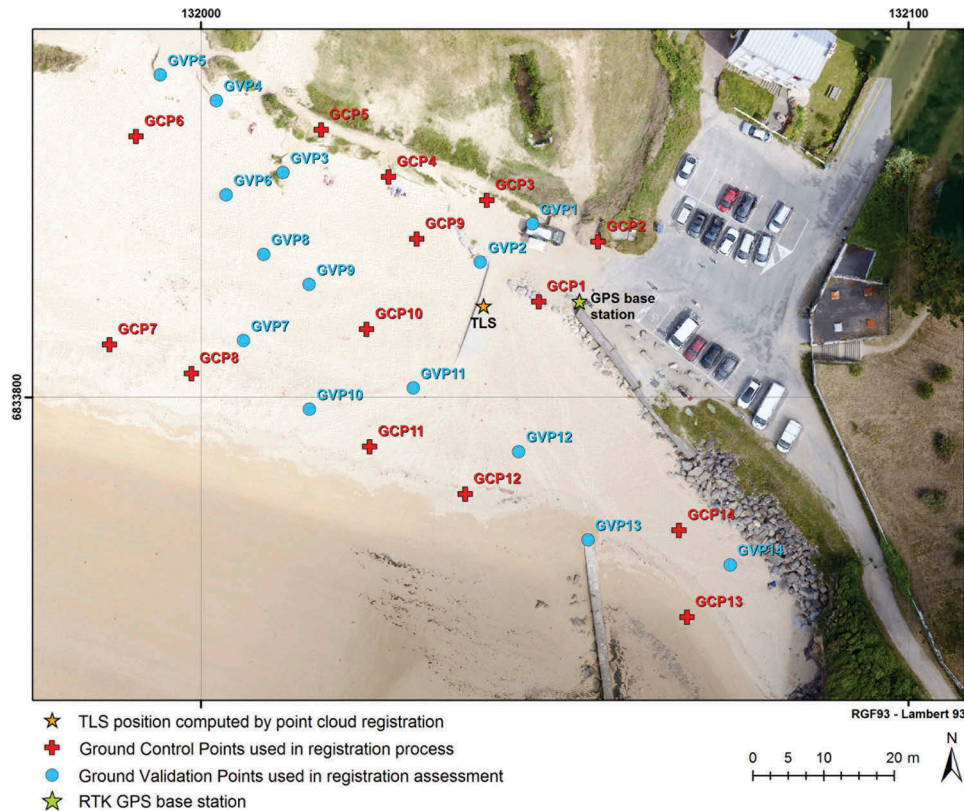


Figure 3. Configuration of the targets for indirect georeferencing.

As integrated compasses are generally not accurate enough to measure the azimuth orientation, it is then performed by aligning the scanner head along a known direction via the measurement of a tie point. This approach is called “backsighting”.

The aforementioned challenge in creating permanent known positions in a coastal setting applies to the scanner station as well. The position of the TLS has therefore to be measured at each survey. As was also mentioned by Scaioni (2005), the quality of the parts supplied by TLS vendors for direct georeferencing is generally inadequate for high accuracy applications. The roll and pitch parameters are measured by internal inclination sensors with a precision of $\pm 0.01^\circ$, which can induce errors of 1.7 cm at a range of 100 m. The yaw angle, corresponding to the heading parameter, is measured by an integrated compass with a typical accuracy of 1° , which can generate errors up to 1.75 m at a range of 100 m. Several repetitive tests have shown that the internal sensors are in reality less precise than the typical accuracy values specified by the manufacturer. The internal position sensor of our instrument (Riegl VZ-400) is an autonomous GPS L1 receiver. Tests show an uncertainty around 2.5 m with eight satellites in view, which is insufficient. Since these results do not meet our accuracy requirements, we propose an alternative method with a straightforward and time-efficient protocol.

We use the dedicated adapter on our TLS to mount an external GPS antenna, a Topcon RTK GNSS receiver, overtop, as shown in Figure 4. The TLS position is thus measured by differential RTK GPS, with centimeter accuracy. The offsets between the GPS antenna center and the scanner center (Figure 4(b)) are extracted from the technical data-sheets: the vertical offset is 34.99 cm and the horizontal offset along X-axis is 1.85 cm.

In this configuration, the TLS tripod mounting platform has been coarsely leveled ($\pm 1^\circ$). Here, it is not necessary to measure the height of the TLS nor that of the GPS antenna, since the position of the scanner center is directly obtained from the measured GPS antenna position. Before the rotation of the scanner, RTK GPS measurements of the scanner position are collected during 5 min.

Roll and pitch angles are measured by the internal inclinometers. The azimuth (yaw angle) is computed using backsighting techniques. For this purpose, the only reflective target used as GCP, called backsight target, is measured by RTK GPS during 2 min. To avoid operator-induced measurement uncertainty, the GPS rover pole can be held on position on a bipod (Figure 5). The sole target is placed about 55 m away from the TLS standpoint (Figure 6), within unobstructed view of the TLS and the satellites. Since the standard deviation of the scanner azimuth is inversely proportional to the distance to the backsight target (Reshetyuk, 2009), choosing a

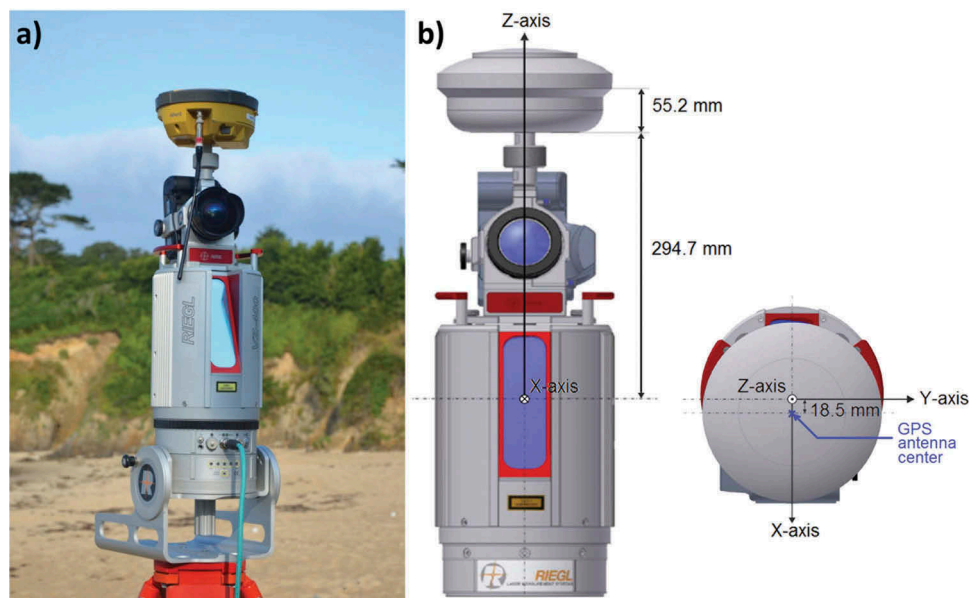


Figure 4. (a) Riegl® VZ-400 TLS equipped with a Nikon D200 camera and a Topcon GNSS antenna. (b) Dimensioned front and top views of the coupled TLS, camera and GPS antenna.



Figure 5. Backsight target accurately measured by RTK GPS, with GPS pole held by an adjustable bipod.

sufficiently large distance is important to reduce the associated error. However, automatic identification of the target centroid can be less accurate if the backsight target is too far from the TLS.

The other 27 reflective targets (Figure 6) are used as GVPs to assess the registration accuracy.

This method is quite convenient since neither the coordinates of the TLS station position nor the

coordinates of the backsight target have to be known *a priori*. Moreover, using only one target yields a significant gain in survey time. It makes also the logistic of the survey easier, because there are fewer targets to carry to the different standpoints distributed over the scanning site, fine scan and measure with RTK GPS.

Results and discussion

Table 1 shows the comparisons between the TLS center positions deduced from GPS measurements and computed by indirect georeferencing. The root mean square (RMS) error between these positions is 0.9 cm. Given our accuracy expectation on the order of a few centimeters, this result fulfills the requirements.

Then, the absolute accuracy of the results is assessed using the set of GVPs. Because these GVPs are reflective targets which are not taken into account in the registration process, 14 GVP are available to assess indirect georeferencing, while 27 GVPs (by adding 13 control points from the GCPs used in the case of indirect georeferencing) are available for pseudo-direct georeferencing. The error budget computed from the GVPs can arise from georeferencing method errors, as well as from intrinsic TLS measurement errors, and GPS errors when measuring the GVPs position. Results are presented in Table 2. These RMS errors are both of the order of magnitude of the RTK GPS error. On average, the RMS error for the indirect georeferencing approach is 4.4 cm, whereas the average RMS error for the pseudo-direct georeferencing approach is 3.8 cm (Table 2). The uncertainty of both indirect and pseudo-direct georeferencing methods appears to be very similar, with

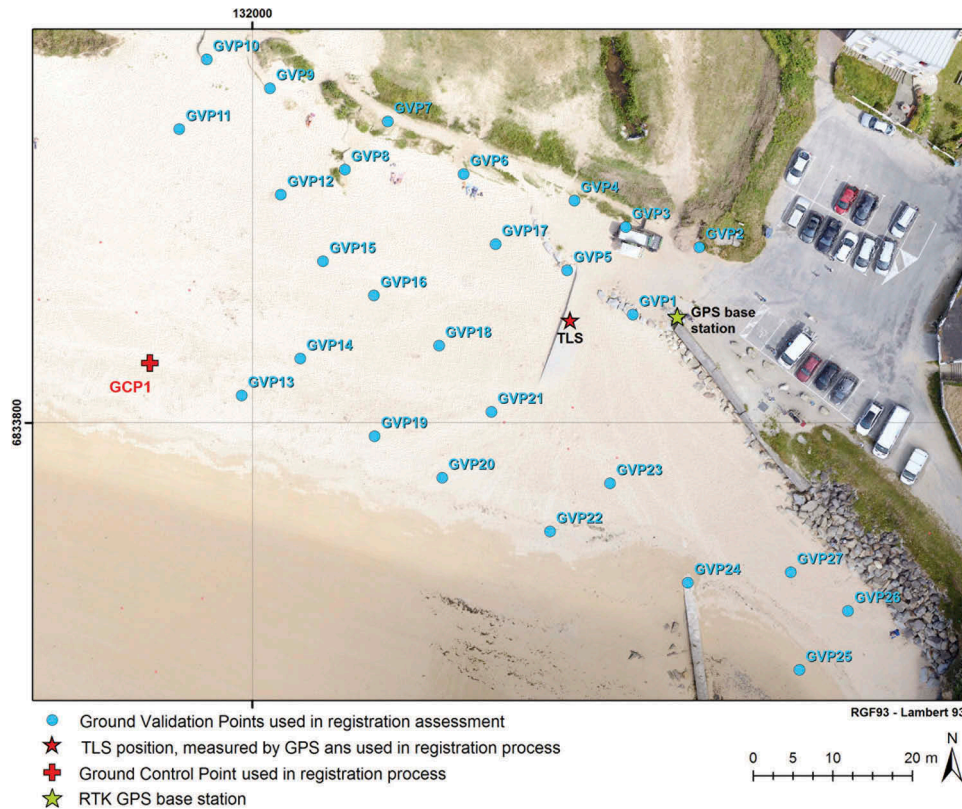


Figure 6. Configuration of the targets for pseudo-direct georeferencing.

Table 1. Comparison of the position of the TLS center computed with the different georeferencing methods.

TLS position computed by indirect georeferencing	TLS position measured by RTK GPS
$X_{TLS} = 132039.928$ m	$X_{TLS} = 132039.927$ m
$Y_{TLS} = 6833812.888$ m	$Y_{TLS} = 6833812.879$ m
$Z_{TLS} = 7.002$ m	$Z_{TLS} = 6.989$ m

Table 2. Georeferencing uncertainty computed for the ground validation points (GVPs).

Indirect georeferencing RMS error computed on 14 GVP	Pseudo-direct georeferencing RMS error computed on 27 GVP
$X_{RMS} = 4.4$ cm	$X_{RMS} = 3.6$ cm
$Y_{RMS} = 2.5$ cm	$Y_{RMS} = 2.5$ cm
$Z_{RMS} = 6.3$ cm	$Z_{RMS} = 5.3$ cm
Total RMS = 4.7 cm	Total RMS = 4.0 cm

errors of a few centimeters. Horizontal positioning error is lower than vertical error, which is consistent with the fact that RTK GPS error is lower horizontally than vertically.

As the registration error can be anisotropic and may not be spatially uniform (Lague et al., 2013), point-wise assessment of the error may be insufficient. The point clouds registered by pseudo-direct georeferencing and indirect georeferencing were compared relative to each other. Both point clouds being affected by the same intrinsic TLS measurement errors, only the differences between both georeferencing methods are thus taken into account. The “cloud-to-cloud” distance was computed in

CloudCompare© (Telecom ParisTech - EDF, France). The mean cloud-to-cloud distance between the clouds registered by both georeferencing methods, pseudo-direct and indirect, is 2.9 cm with a standard deviation of 4.2 cm.

The different error assessments (comparative and absolute) are quite consistent, with the cloud-to-cloud distance and the absolute accuracy of the measurements of the same order. The former is slightly lower than the latter meaning that the difference in output between both georeferencing methods is smaller than the intrinsic error of either method.

Within the overall error budget, the present study is addressing the georeferencing error. The uncertainty of registration is mainly due to the uncertainty in target position measurements. The indirect georeferencing method is less affected by target measurement errors than the pseudo-direct georeferencing method due to GCPs redundancy in the indirect georeferencing method. The configuration of the GCPs network by the survey operator and the quality of the automatic target detection within the point cloud, performed by the data acquisition software, can also affect the georeferencing uncertainty. The main drawback of this method is the time-consuming procedure consisting in laying out the targets, taking a GPS measurement of their position and performing a fine-scan with the TLS.

On the opposite, the pseudo-direct georeferencing approach is very quick since the same steps are required

for only one target. To shorten surveying time is critical in the coastal environment where survey plans tend to require accommodating for the tide schedule, as well as under certain climates where favorable weather windows can be quite brief. Naturally, this method is highly dependent on the accuracy of the position measurement for the TLS center and the backsight target. The cloud-to-cloud mean distance between the unbiased and biased point clouds is 1.8 cm, with a standard deviation of 3.3 cm. The distribution of the error is very uneven: the points close to the TLS (where the point cloud is denser) are nearly not affected (less than 1 cm of error up to 10 m from the TLS), while the positioning error for the farthest points (up to 400 m) reach up to 6 m. Depending on the satellite configuration, the observation time of the backsight target may be increased in order to improve the accuracy of the position measurement of the backsight target. For example, introducing an error of 5 cm in the northing position of the backsight target (situated 55 m away from the TLS) induces an error of 0.05° in the estimation of yaw angle, and thus a bias in the point cloud georeferencing.

Figure 7(a) shows the effects of (1) positioning errors of the single backsight target and of (2) the distance between TLS and the target on the estimation of heading angle. It appears that the farther is the backsight target, the better is the estimation of heading angle. But the farther the TLS, the less accurate is the automatic estimation of the target center in the TLS point cloud. Considering that the TLS precision is 3 mm at 100 m of range (RIEGL VZ-400), and the spatial resolution of the fine-scan of the target given by Figure 7(b), the impact of the relative positioning of the target centroid in the point cloud is negligible compared to GPS positioning errors. Nevertheless, placing the backsight target far from the TLS, it is recommended to use a bigger target.

In this study, the TLS tripod mounting platform is coarsely leveled, about $\pm 1^\circ$. Due to the small vertical offset (34.9 cm) between the GPS antenna and the TLS center,

more accurate leveling does not appear necessary at this stage. Indeed, a 1° error in platform tilt induces 6 mm of uncertainty in TLS center positioning. Such uncertainty is acceptable since it is lower than RTK GPS accuracy. The measurement of the platform tilt does not impact the rotation matrix R (Equation (3)) since the roll and pitch angles are measured by the internal inclinometers.

In theory, 3D positioning of one backsight target yields not only the azimuth angle ψ but also the pitch angle θ . Considering both the RTK GPS accuracy and the uncertainty on TLS automatic target centroid detection and comparing with the internal inclinometers accuracy, it appears preferable to use the pitch value from the inclinometer when available. Nevertheless, the pseudo-direct georeferencing method may still be used with TLS which are not equipped with internal sensors, provided that the TLS platform is precisely leveled (i.e. in this configuration, $\varphi = \theta = 0$). Then, RTK GPS measurements of the TLS center and of one backsight target are sufficient for direct georeferencing of the point cloud. It is also possible to carry out the Survey without internal inclinometer or precise leveling of the platform, but by using two backsight targets in order to obtain the roll, pitch and yaw angles.

The pseudo-direct georeferencing method is proposed in this study for a single TLS station survey. It can be reproduced for each TLS station, with DGPS measurement of the TLS position and measurement of the backsight target position. Nevertheless, to optimize fieldwork when several TLS stations are needed, the same backsight target can be used for several scans. The backsight target has so to be placed so as to be seen from the different TLS stations. Figure 8 provides some guidance to optimize the fieldwork for multi-station survey in linear and nonlinear context. The position of the TLS (X_{TLS} , Y_{TLS} , Z_{TLS}) has to be measured at each station; however, it may be not necessary to create a backsight target for each station.

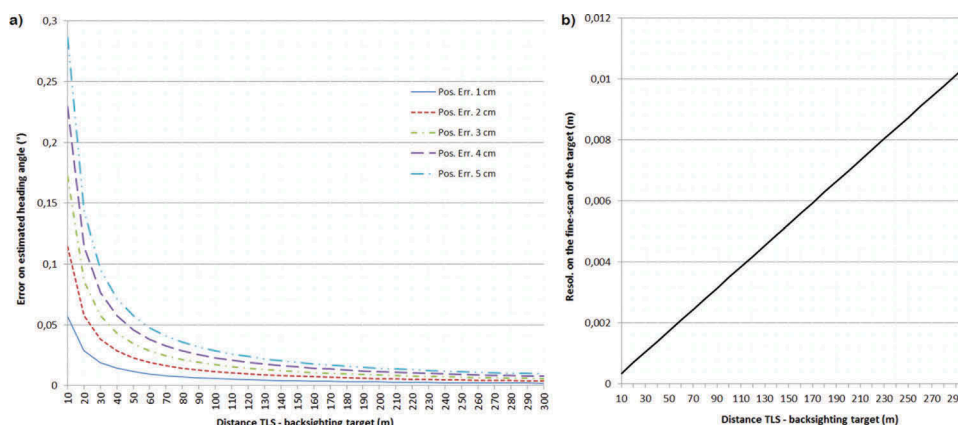


Figure 7. (a) Impact of the positioning error of the backsight target (from 1 to 5 cm) and of the distance between the TLS and the backsight target on the estimation of the heading angle. (b) Impact of the distance between the TLS and the backsight target on the resolution of the fine-scan of the backsight target.

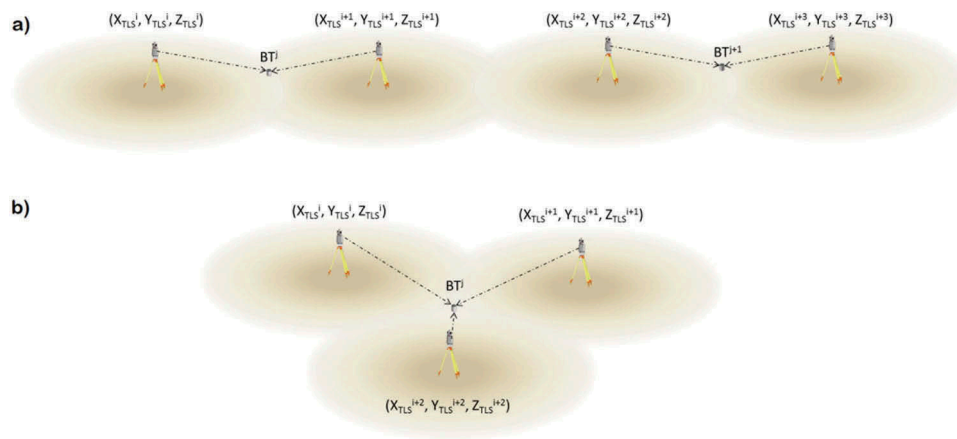


Figure 8. Guidance to optimize fieldwork for multi-station survey with pseudo-direct georeferencing in linear (a) and nonlinear (b) contexts. BT is the position of the backsight target. At each station, the position of the TLS (X_{TLS} , Y_{TLS} , Z_{TLS}) has to be measured.

Conclusion

High-resolution and high-accuracy data from TLS surveys are now commonplace in coastal monitoring. A well-defined acquisition procedure can significantly shorten surveying time, which can be critical again in the coastal environment. The choice of the georeferencing method depends on (1) the accuracy required and (2) the constraints imposed by the study area.

This paper assesses the performance of a field protocol aimed at reducing survey time without increasing georeferencing errors.

Considering the suboptimal quality of the internal sensors supplied by vendors, it is not possible to carry out real-time direct georeferencing. Consequently, a pseudo-direct georeferencing method is proposed. The protocol involves internal inclinometers to measure roll and pitch angles and a RTK GPS to measure the position of the TLS center and the position of one backsight target. This method is much quicker than classical indirect georeferencing. The cloud-to-cloud mean distance resulted in 2.9 cm, while the intrinsic error is lower for the pseudo-direct georeferencing method. Assessing the accuracy of each method with GVPs, we get an average RMS error of 4.4 cm for classical indirect georeferencing, and of 3.8 cm for pseudo-direct georeferencing. Accordingly, despite the low redundancy of the pseudo-direct georeferencing method (only two points are positioned through the RTK technique, the TLS center and the backsight target), this method proved to be more precise than the indirect georeferencing approach.

Acknowledgments

This work was supported by the “Laboratoire d’Excellence” LabexMER (ANR-10-LABX-19) and co-funded by a grant from the French government under the program “Investissements d’Avenir”.

Disclosure statement

No potential conflict of interest was reported by the authors.

Funding

This work was supported by the “Laboratoire d’Excellence” LabexMER [ANR-10-LABX-19] and co-funded by a grant from the French government under the program “Investissements d’Avenir”.

ORCID

Marion Jaud  <http://orcid.org/0000-0002-7629-9710>

References

- Abellán, A., Oppikofer, T., Jaboyedoff, M., Rosser, N.J., Lim, M., & Lato, M.J. (2014). Terrestrial laser scanning of rock slope instabilities. *Earth Surface Processes and Landforms*, 39(1), 80–97. doi:10.1002/esp.v39.1
- Alba, M., Giussani, A., Roncoroni, F., & Scaioni, M. (2007). Review and comparison of techniques for terrestrial 3D-View georeferencing. In *Proceedings of the 5th International Symposium on Mobile Mapping Technology (ISPRS)*. Padua, Italy.
- Alba, M., & Scaioni, M. (2007). Comparison of techniques for terrestrial laser scanning data georeferencing applied to 3-D modelling of cultural heritage. *The International Archives of the Photogrammetry, Remote Sensing and Spatial Information Sciences*, 36, XXXVI-5/W47.
- Alho, P., Vaaja, M., Kukko, A., Kasvi, E., Kurkela, M., Hyypä, J., ... Kaartinen, H. (2011). Mobile laser scanning in fluvial geomorphology: Mapping and change detection of point bars. *Zeitschrift Für Geomorphologie*, 55, 31–50. doi:10.1127/0372-8854/2011/0055S2-0044
- Barber, D., Mills, J., & Smith-Voysey, S. (2008). Geometric validation of a ground-based mobile laser scanning system. *ISPRS Journal of Photogrammetry and Remote Sensing*, 63, 128–141. doi:10.1016/j.isprsjprs.2007.07.005
- Besl, P.J., & McKay, N.D. (1992). A method for registration of 3-D shapes. *IEEE Transactions on Pattern Analysis*

- and Machine Intelligence, 14(2), 239–256. doi:10.1109/34.121791
- Bitelli, G., Dubbini, M., & Zanutta, A. (2004). Terrestrial laser scanning and digital photogrammetry techniques to monitor landslide bodies. In *Proceedings of the XXth ISPRS Congress Geo-Imagery Bridging Continents*. International Society of Photogrammetry and Remote Sensing (ISPRS), Istanbul, Turkey.
- Cuartero, A., Armesto, J., Rodríguez, P.G., & Arias, P. (2010). Error analysis of terrestrial laser scanning data by means of spherical statistics and 3D graphs. *Sensors*, 10, 10128–10145. doi:10.3390/s101110128
- Delacourt, C., Allemand, P., Jaud, M., Grandjean, P., Deschamps, A., Ammann, J., ... Suanez, S. (2009). DRELIO: An unmanned helicopter for imaging coastal areas [Special issue]. *Journal of Coastal Research*, 56, 1489–1493. doi:10.2307/25738037
- Earlie, C.S., Young, A.P., Masselink, G., & Russell, P.E. (2015). Coastal cliff ground motions and response to extreme storm waves. *Geophysical Research Letters*, 42 (3), 847–854. doi:10.1002/2014GL062534
- Giussani, A., & Scaioni, M. (2004). Application of TLS to support landslides study: Survey planning, operational issues and data processing. *International Archives of Photogrammetry, Remote Sensing and Spatial Information Sciences*, 36, 318–323.
- Harwin, S., & Lucieer, A. (2012). Assessing the accuracy of georeferenced point clouds produced via multi-view stereopsis from unmanned aerial vehicle (UAV) imagery. *Remote Sensing*, 4, 1573–1599. doi:10.3390/rs4061573
- Jaud, M., Delacourt, C., Allemand, P., Deschamps, A., Cancouët, R., Ammann, J., & Cuq, V. (2011, December). *Comparison of some very high resolution remote sensing techniques for the monitoring of a sandy beach*. Poster session presented at the AGU Fall Meeting, San Francisco, CA.
- Kasperski, J., Delacourt, C., Allemand, P., Potherat, P., Jaud, M., & Varrel, E. (2010). Application of a terrestrial laser scanner (TLS) to the study of the Séchilienne landslide (Isère, France). *Remote Sensing*, 2, 2785–2802. doi:10.3390/rs122785
- Kuhn, D., & Prüfer, S. (2014). Coastal cliff monitoring and analysis of mass wasting processes with the application of terrestrial laser scanning: A case study of Rügen, Germany. *Geomorphology*, 213, 153–165. doi:10.1016/j.geomorph.2014.01.005
- Kukko, A., Kaartinen, H., Hyyppä, J., & Chen, Y. (2012). Multiplatform mobile laser scanning: Usability and performance. *Sensors*, 12, 11712–11733. doi:10.3390/s120911712
- Lague, D., Brodu, N., & Leroux, J. (2013). Accurate 3D comparison of complex topography with terrestrial laser scanner: Application to the Rangitikei canyon (N-Z). *ISPRS Journal of Photogrammetry and Remote Sensing*, 82, 10–26. doi:10.1016/j.isprsjprs.2013.04.009
- Leroux, J. (2013). *Chenaux tidaux et dynamique des prés-salés en régime méga-tidal: Approche multi-temporelle du siècle à l'événement de marée*. (Doctoral dissertation, Université Rennes 1 - Université Européenne de Bretagne, Rennes, France). Retrieved from <https://tel.archives-ouvertes.fr/tel-01005360/>
- Letortu, P., Costa, S., Maquaire, O., Delacourt, C., Augereau, E., Davidson, R., ... Nabucet, J. (2015). Retreat rates, modalities and agents responsible for erosion along the coastal chalk cliffs of Upper Normandy: The contribution of terrestrial laser scanning. *Geomorphology*, 245, 3–14. doi:10.1016/j.geomorph.2015.05.007
- Lichti, D.D., & Gordon, S.J. (2004). Error propagation in directly georeferenced terrestrial laser scanner point clouds for cultural heritage recording. In *The proceedings of FIG Working Week*. International Federation of Surveyors, Athens, Greece.
- Lim, M., Dunning, S.A., Burke, M., King, H., & King, N. (2015). Quantification and implications of change in organic carbon bearing coastal dune cliffs: A multiscale analysis from the Northumberland coast, UK. *Remote Sensing of Environment*, 163, 1–12. doi:10.1016/j.rse.2015.01.034
- Mancini, F., Dubbini, M., Gattelli, M., Stecchi, F., Fabbri, S., & Gabbianelli, G. (2013). Using unmanned aerial vehicles (UAV) for high-resolution reconstruction of topography: The structure from motion approach on coastal environments. *Remote Sensing*, 5, 6880–6898. doi:10.3390/rs5126880
- Mårtensson, S.G., Reshetyuk, Y., & Jivall, L. (2012). Measurement uncertainty in network RTK GNSS-based positioning of a terrestrial laser scanner. *Journal of Applied Geodesy*, 6, 25–32. doi:10.1515/jag-2011-0013
- Nield, J.M., Wiggs, G.F., & Squirrell, R.S. (2011). Aeolian sand strip mobility and protodune development on a drying beach: Examining surface moisture and surface roughness patterns measured by terrestrial laser scanning. *Earth Surface Processes and Landforms*, 36(4), 513–522. doi:10.1002/esp.2071
- Olsen, M., Johnstone, E., Driscoll, N., Ashford, S., & Kuester, F. (2009). Terrestrial laser scanning of extended cliff sections in dynamic environments: Parameter analysis. *Journal of Surveying Engineering*, 135(4), 161–169. doi:10.1061/(ASCE)0733-9453(2009)135:4(161)
- Olsen, M., Johnstone, E., Kuester, F., Driscoll, N., & Ashford, S. (2011). New automated point-cloud alignment for ground-based light detection and ranging data of long coastal sections. *Journal of Surveying Engineering*, 137(1), 14–25. doi:10.1061/(ASCE)SU.1943-5428.0000030
- Paffenholz, J.-A. (2012). *Direct geo-referencing of 3D point clouds with 3D positioning sensors* (Doctoral dissertation, Deutsche Geodätische Kommission (DGK) in the Bayrischen Akademie der Wissenschaften, München, Germany). Retrieved from <https://www.researchgate.net/>
- Pietro, L.S., O'Neal, M.A., & Puleo, J.A. (2008). Developing terrestrial-LIDAR-based digital elevation models for monitoring beach nourishment performance. *Journal of Coastal Research*, 24(6), 1555–1564. doi:10.2112/07-0904.1
- Quinn, J.D., Rosser, N.J., Murphy, W., & Lawrence, J.A. (2010). Identifying the behavioural characteristics of clay cliffs using intensive monitoring and geotechnical numerical modelling. *Geomorphology*, 120(3), 107–122. doi:10.1016/j.geomorph.2010.03.004
- Reshetyuk, Y. (2009). *Self-calibration and direct georeferencing with GPS in terrestrial laser scanning* (Doctoral dissertation, Royal Institute of Technology (KTH), Stockholm, Sweden). Retrieved from <http://citeseerx.ist.psu.edu/>
- RIEGL VZ-400. 3D Terrestrial Laser Scanner RIEGL VZ-400 /RIEGL VZ-1000 (version 03/09 CE – Rev. 10/11/2014).
- Rosser, N.J., Brain, M.J., Petley, D.N., Lim, M., & Norman, E.C. (2013). Coastline retreat via progressive failure of rocky coastal cliffs. *Geology*, 41(8), 939–942. doi:10.1130/G34371.1
- Rosser, N.J., Petley, D.N., Lim, M., Dunning, S.A., & Allison, R.J. (2005). Terrestrial laser scanning for

- monitoring the process of hard rock coastal cliff erosion. *Quarterly Journal of Engineering Geology and Hydrogeology*, 38(4), 363–375. doi:[10.1144/1470-9236/05-008](https://doi.org/10.1144/1470-9236/05-008)
- Scaioni, M. (2005). Direct georeferencing of TLS in surveying of complex sites. In *The Proceedings of the ISPRS Working Group V/4 Workshop 3D-ARCH “Virtual Reconstruction and Visualization of Complex Architectures”*. International Society of Photogrammetry and Remote Sensing (ISPRS), Mestre-Venice, Italy.
- Schubert, J.E., Gallien, T.W., Majd, M.S., & Sanders, B.F. (2015). Terrestrial laser scanning of anthropogenic beach berm erosion and overtopping. *Journal of Coastal Research*, 31(1), 47–60. doi:[10.2112/JCOASTRES-D-14-00037.1](https://doi.org/10.2112/JCOASTRES-D-14-00037.1)
- Schürch, P., Densmore, A.L., Rosser, N.J., Lim, M., & McArdell, B.W. (2011). Detection of surface change in complex topography using terrestrial laser scanning: Application to the Illgraben debris-flow channel. *Earth Surface Processes and Landforms*, 36(14), 1847–1859. doi:[10.1002/esp.2206](https://doi.org/10.1002/esp.2206)